

Disorder Induced Negative Magnetization in LaSrCoRuO_6

P. S. R. Murthy ^a, K. R. Priolkar ^{a,*}, P. A. Bhobe ^b, A. Das ^c,
P. R. Sarode ^a and A. K. Nigam ^b

^a*Department of Physics, Goa University, Goa, 403 206 India.*

^b*Tata Institute of Fundamental Research, Homi Bhabha Road, Mumbai, 400 005 India*

^c*Solid State Physics Division, Bhabha Atomic Research Centre, Trombay, Mumbai 400 085 India*

Abstract

This paper reports effect of thermally induced disorder on the magnetic properties of LaSrCoRuO_6 double perovskite. While the ordered sample is antiferromagnetic, the disordered sample exhibits negative values of magnetization measured in low applied fields. Isothermal magnetization on this sample shows hysteresis due to presence of ferromagnetic interactions. Based on neutron diffraction and X-ray Absorption Fine Structure (XAFS) studies, these results have been interpreted to be due disorder in site occupancy of Co and Ru leading to octahedral distortions and formation of Ru-O-Ru ferromagnetic linkages. Below 150K these ferromagnetic Ru spins polarize the Co spins in a direction opposite to that of the applied field resulting in observed negative magnetization.

Key words:

PACS: 72.15.Jf; 81.30.Kf; 75.50.Cc

1 Introduction

Ordering of B-site cations in the double perovskites is known to play an important role in deciding the magnetic, transport and structural properties of these systems. $\text{Sr}_2\text{FeMoO}_6$ and $\text{Sr}_2\text{FeReO}_6$ both of which display large low

* Corresponding author

Email address: krp@unigoa.ac.in (K. R. Priolkar).

field magnetoresistance are two good examples [1,2]. The itinerancy and ferrimagnetism in the above materials arise from a double exchange type of mechanism in which the ordering and electronic configurations play a critical role [3]. The characteristics of this type of ordering stems from the fact that it combines features of both ferromagnetic (FM) and antiferromagnetic (AF) systems. Moreover, if more than two spin sub-lattices are involved, a new phenomena like temperature induced magnetization reversal can emerge [4]. So far, apart from ferrimagnets [5] only few other families of oxides which include layered ruthenates and manganites have exhibited temperature induced magnetization reversal [4,6,7,8,9,10,11,12].

The layered compounds, often characterized by a strong competition between antiferromagnetic and ferromagnetic coupling and a complex interplay of spin, charge, and orbital degrees of freedom, are extremely sensitive to small perturbations such as slight structural alterations. Sr_2YRuO_6 is a typical example. Here the negative magnetization observed in low fields has been ascribed to two oppositely ordered ferromagnetic superexchange interactions viz, Ru-O-O-Ru and Ru-O-Y-O-Ru [10]. LaSrCoRuO_6 is a type of layered compound wherein degree of B-site (Co and Ru) order can lead to intriguing magnetic and transport properties [13,14]. However, here unlike Y, Co is a magnetic ion and that has led to different interpretations of the nature of magnetic order in this compound. LaSrCoRuO_6 was reported to be a 3D variable range hopping semiconductor with magnetic ordering temperature of 157K [15]. Recent studies suggest that the compound is an antiferromagnet with $T_N = 87\text{K}$ [13] or a spin glass [14] and the transition at 157K could be due to SrRuO_3 impurity. Apart from SrRuO_3 impurity phase, the sharp rise in magnetization can also be due to ferromagnetic Ru-O-Ru interactions arising from antiphase grain boundaries [16]. The studies conducted on LaSrCoRuO_6 so far by varying the composition ratio of A site ions (La and Sr) highlight the importance of different magnetic interactions between $\text{Co}^{2+/3+}$ and $\text{Ru}^{4+/5+}$ in governing the magnetic ground state [14,17]. This paper reports the effect of thermally induced site-occupancy disorder in LaSrCoRuO_6 on its magnetic properties. The most notable feature here is the observation of negative magnetization at low applied fields in the more disordered sample. The results have been explained on the basis of EXAFS data recorded at Co and Ru K-edge to be due to presence of additional ferromagnetic interactions resulting from B-site disorder in an otherwise antiferromagnetic lattice.

2 Experimental

Two polycrystalline samples of LaSrCoRuO_6 were synthesized by solid state reaction method by taking stoichiometric amounts of La_2O_3 , SrCO_3 , $\text{Co}(\text{NO}_3)_2$ and RuO_2 . These starting powders were ground thoroughly, pressed into pel-

lets and heated for a total of 48 hrs, one at 1200°C and the other at 1300°C with three intermediate regrinding steps. The sample annealed at 1200° was quenched to room temperature while the other was furnace cooled. Both the samples were deemed to be phase pure, as X-ray diffraction (XRD) data collected on a Rigaku X-ray diffractometer in the range of $18^\circ \leq 2\theta \leq 80^\circ$ using $\text{CuK}\alpha$ radiation showed no impurity reflections. The diffraction patterns were Rietveld refined using FULLPROF suite and structural parameters were obtained. Scanning Electron Microscopy energy dispersive spectroscopy (SEM EDS) and Iodometric titrations were carried out on these samples to confirm the cation and oxygen stoichiometry. The cation stoichiometries were close the expected value of 10 at.% in case of both the samples. The oxygen stoichiometry in case of 1200°C and 1300°C annealed samples were found to be 5.96 ± 0.02 and 5.99 ± 0.01 respectively. DC magnetization was measured, both, as a function of temperature and magnetic field using the Quantum Design SQUID magnetometer (MPMS-5S). $M(T)$ was measured in an applied field of 50 Oe and 1000 Oe in the temperature range of 5 to 300 K. The sample was initially cooled from 300K to 5 K in zero applied field and the data was recorded while warming up to 300 K in the applied magnetic field (referred to as ZFC curve) and subsequent cooling (referred to as FC curve) back to 5 K. Magnetization as a function of field was measured under sweep magnetic fields up to $\pm 5T$ at various temperatures. Before each $M(H)$ was recorded, the sample was warmed to 300 K and cooled back to the desired temperature. Neutron diffraction (ND) measurements were performed at room temperature (RT) and 20K and a wavelength of 1.24Å using powder diffractometer at Dhruva, Trombay. XAFS experiments at the Co and Ru K edge were performed in transmission mode at room temperature using the beamline 12C at Photon Factory, Tsukuba, Japan.

3 Results and Discussion

The Rietveld refined XRD patterns for two samples of LaSrCoRuO_6 viz, LSCR13 and LSCR12 prepared at 1300°C and 1200°C respectively are presented in Fig. 1. The stoichiometric double perovskite, LaSrCoRuO_6 has a monoclinic structure with the B-site cations Co and Ru ordered in the NaCl pattern in the space group $P2_1/n$. ND patterns recorded at 300K (Fig. 2) show evidence for higher degree of B-site order in LSCR13 as compared to LSCR12. The presence of the sharper $(\frac{1}{2}, \frac{1}{2}, \frac{1}{2})$ super lattice reflection in the ND pattern in LSCR13 (see inset Fig 2) indicates a higher degree of ordering in LSCR13. Rietveld refinement of the XRD and ND patterns was carried out with $P2_1/n$ space group wherein the La/Sr occupy the 4e site with fractional coordinates (0.0033, 0.0218, 0.25), Co is at 2c (0.5, 0, 0.5), Ru is at 2d (0.5, 0, 0) and the oxygen atoms occupy three sites, viz, (0.2886, 0.280,

Table 1

Unit cell parameters, Co and Ru site occupancies obtained from Rietveld refinement and Curie-Weiss parameters calculated from magnetization measurements at 1000 Oe for the two samples of $\text{LaSrCo}_{1-x}\text{Ru}_{1+x}\text{O}_6$. Numbers in parentheses are uncertainty in the last digit.

Sample	LSCR13	LSCR12
a (Å)	5.5847(4)	5.5891(3)
b (Å)	5.5592(6)	5.5540(5)
c (Å)	7.8674(9)	7.8787(5)
β	90.05(2)	90.10(1)
Volume (Å ³)	244.25(4)	244.57(3)
Co ($\frac{1}{2}, 0, \frac{1}{2}$)	0.98(1)	0.87(1)
Ru ($\frac{1}{2}, 0, \frac{1}{2}$)	0.02(1)	0.13(1)
Ru ($\frac{1}{2}, 0, 0$)	0.98(1)	0.87(1)
Co ($\frac{1}{2}, 0, 0$)	0.02(1)	0.13(1)
μ_{eff} (μ_B/fu)	5.47(2)	5.43(1)
$\Theta_{CW}(K)$	-49(2)	-2.5(4)

0.0355); (0.2324, 0.774, 0.0264) and (-0.0662, 0.4938, 0.255) [13]. The scale factor, background parameters, cell parameters, Co and Ru site occupancies along with instrumental broadening, totalling to 17 parameters were refined in that order to obtain a good fit. The crystallographic parameters obtained from refinement of ND patterns along with Curie-Weiss parameters calculated from magnetization measurements are summarized in Table 1. Refinement shows that there is only about 4% disorder in the case of LSCR13 whereas in case of LSCR12 about 20% of Co occupies the Ru site (2d site) and vice versa thereby resulting in a larger disorder in the occupation of the B-sites as compared to LSCR13. Therefore, we refer to LSCR13 as a ordered compound while LSCR12 is referred to as disordered compound.

Magnetization measurements performed at 1000 Oe during the ZFC and FC cycles for the two LaSrCoRuO_6 samples are presented in Fig. 3. In case of LSCR13, both ZFC and FC cycles rise sharply below 160K and branch off below 130K. While the ZFC curve culminates into a broad hump centered at about 55K, the FC curve approaches a constant value below 77K. These curves do not reveal the nature of magnetic order in the compound. It may be noted here that spin frozen ground state has been previously reported for this composition [14]. In yet another study, antiferromagnetic order has also been have reported with $T_N = 87\text{K}$ [13]. In order to confirm the nature of magnetic order in the present sample, ND pattern was recorded at 20K and is presented in Fig. 2. Weak extra reflections due to antiferromagnetic ordering

are seen at the positions described by propagation vector along the $k = \frac{1}{2} 0 \frac{1}{2}$ with respect to the crystallographic $P2_1/n$ cell. This magnetic arrangement is the same as that reported by Bos and Attfield [13].

In the case of LSCR12 there is a wide difference in magnetization behaviour recorded during ZFC and FC cycles. The ZFC magnetization with increasing temperature increases sharply culminating into a broad hump centred around 50K. It decreases slightly with further rise in temperature before increasing sharply resulting in a peak at 151K. The FC magnetization, on the other hand decreases continuously to 167K and settles into a low value giving an impression of ferro to para transition. The differences in behaviour of magnetization during ZFC and FC cycle indicates a complex magnetic ground state. ND pattern recorded at 20K also does not show any evidence of long range magnetic order within our detectable limit. This could be implied to a magnetically frustrated ground state due to presence of competing ferro and antiferromagnetic interactions.

Plot of inverse of susceptibility ($1/\chi = H/M$) in Fig. 4. For LSCR13 $1/\chi$ varies linearly with temperature in the range $170K < T < 300K$ and Curie-Weiss fit to the data yields effective paramagnetic moment $\mu_{eff} = 5.47 \mu_B/\text{f.u.}$ in good agreement with the calculated spin only moment of Co^{2+} and Ru^{5+} ions and the Curie-Weiss temperature, $\Theta_{CW} = -49K$ that is also in good agreement with the value reported earlier [14]. The negative Θ_{CW} indicates presence of strong antiferromagnetic interactions. In the case of LSCR12, the susceptibility although seems to be fairly linear down to 170K, deviates below the Curie-Weiss behaviour at temperatures less than 220K. A linear fit in the temperature region 300K to 240K, to inverse susceptibility of LSCR12 with Curie-Weiss equation results in $\mu_{eff} = 5.43\mu_B/\text{f.u.}$ and $\Theta_{CW} = -2.5K$ (see Fig. 4). The reduced value of Θ_{CW} and the deviation from Curie-Weiss behaviour from higher temperature in LSCR12 points to presence of short range ferromagnetic interactions in this compound. The presence of ferromagnetic interactions can be due to presence of small amount of SrRuO_3 impurity which has an ordering temperature in the region of 140K - 160K. Although this agrees well with the sharp rise in magnetization in LSCR12 below 170K, the deviation of susceptibility from Curie-Weiss behaviour from about 220K hints at the presence of short range ferromagnetic interactions arising due to some other reason than due to SrRuO_3 impurity alone. Further the absence of magnetic Bragg reflections in the neutron diffraction pattern of LSCR12 due to antiferromagnetic order as in case of LSCR13 emphasize the presence of short range ferromagnetic interactions within LaSrCoRuO_6 lattice. Presence of small amounts of SrRuO_3 impurity would not alter the magnetic ground state of parent LaSrCoRuO_6 .

In order to understand magnetic properties better, the low field (50 Oe) magnetization data were measured during ZFC and FC cycles on the two samples

of LaSrCoRuO_6 and are presented in Fig. 5. In case of LSCR12, magnetization measured during the ZFC cycle is negative at the lowest temperature. It decreases in magnitude with increasing temperature and crosses over to the positive side at 155 K, exhibits a peak at 160 K signifying a transition from a magnetically ordered to paramagnetic state. During the FC cycle, magnetization behaviour is similar except its value is positive throughout. Such a behaviour again cannot be understood to be due to presence of SrRuO_3 impurity alone. It may be emphasized here that care has been taken to make sure that the remanent field of SQUID magnetometer was less than ± 13 Oe during these low field measurements. In case of LSCR13, although the magnetization exhibits significant deviation between ZFC and FC cycles below 160K but is positive throughout.

Isothermal magnetic response of the two samples has been studied at various temperature in the field range of ± 50 KOe. Fig. 6(a) presents the isothermal magnetization curve for LSCR13 measured at 5K. The amplified loop (± 10 KOe) is presented in Fig. 6(b). It can be seen that the magnetization exhibits strong field dependency and almost no hysteresis which is typical of an antiferromagnet. On the other hand for LSCR12 the isothermal magnetization studies performed at 5K (see Fig. 7(a)) exhibit a clear ferromagnetic hysteresis loop riding on an antiferromagnetic (linear) background. Such a hysteresis loop is typical for a compound with a ferromagnetic component along with antiferromagnetic interactions. The expanded loop in Fig. 7(b) shows that the ferromagnetic component is quite strong and about 4 to 5 times larger than that reported in Ref. [13]. Calculation of saturation moment by extrapolating the linear regions of hysteresis loop yields a value of 0.64 emu/gm which is about 6% of the value of Ru in SrRuO_3 . This cannot be ascribed to SrRuO_3 impurity alone as such a sizeable amount of SrRuO_3 would have been detected in diffraction studies. Therefore the observed magnetic behaviour can only be ascribed to presence of competing ferromagnetic and antiferromagnetic interactions resulting due to higher B-site disorder present in LSCR12. As the low field magnetization measured in ZFC cycle is negative, it is worthwhile to see the behaviour of virgin magnetization at different temperatures especially in the low field region. Fig. 7(c) exhibits the virgin magnetization curves for LSCR12 and Fig. 6(c) presents the same for LSCR13. While the magnetization remains positive even very low fields for LSCR13, corresponding magnetization for LSCR12 is negative. Further the shape of virgin curve at 100K makes it amply clear that ferromagnetism is more dominant while the 5K curve is more linear corresponding to dominant antiferromagnetic interactions. This again excludes the possibility of ferromagnetism arising due to SrRuO_3 impurity alone. Further, in case of LSCR12, the value of magnetization at a low field (~ 50 Oe) extracted from virgin curves decreases below 150K and then shows a upturn towards positive values below 80K. This is more clearly depicted in Fig. 7(d). This clearly points to a presence of two magnetic sublattices which interact with each other leading to observed negative magnetization. No such

Table 2

Structural parameters like bond length (R \AA), bond angle and mean square radial displacement ($\sigma^2\text{\AA}^2$) obtained from Co and Ru K edge EXAFS analysis. Numbers in parentheses are uncertainty in the last digit.

Bond	LSCR13		LSCR12	
	R (\AA)	σ^2 (\AA^2)	R (\AA)	σ^2 (\AA^2)
Co-O	2.054(7)	0.008(1)	2.046(9)	0.009(1)
Ru-O	1.967(8)	0.003(1)	1.950(5)	0.004(1)
Co-Ru	3.97(6)	0.002(1)	3.97(1)	0.005(1)
Co-Ru-O-Co	4.00(7)	0.002(1)	4.00(1)	0.004(1)
\angle Co-O-Ru	161.7(1) $^\circ$		166.4(1) $^\circ$	

dependence is observed in case of LSCR13 (see Fig. 6(d)).

A disorder in site occupancy of Co and Ru sites can strengthen ferromagnetic interactions. Such a disorder can result in Ru-O-Ru networks which will alter the Co and Ru octahedral networks, especially the Co-O-Ru bond angle. In order to investigate the changes in the local structures around Co and Ru in between the two samples, respective EXAFS data has been analyzed and the results are presented in Table 2 and Fig. 8. It can be seen from the Table that in case of LSCR12 the Co-O and Ru-O bond lengths are lower and the mean square radial displacements (σ^2) are higher as compared to those in LSCR13. Further, the values of Co-Ru single scattering bond length and Co-O-Ru multiple scattering bond length indicate that the Co-O-Ru bond angle increases in LSCR12 as compared to LSCR13. A straighter Co(Ru)-O-Ru(Co) bond angle implies a formation of quasi-itinerant π^* bands of Ru and/or ferromagnetic superexchange of high spin Co^{2+} -O-Ru $^{5+}$ type. The higher value of σ^2 for Co-Ru bond distance are indicative of larger disorder in LSCR12. These local structural changes can be understood to be due to B-site occupancy disorder in LSCR12 resulting in formation of π^* bands due to Ru-O-Ru linkages. These itinerant-electron π^* bands interact ferromagnetically which explains the sudden increase in magnetization below 150K. The ferromagnetic Ru sublattice so formed is coupled by an antiferromagnetic exchange interaction to the Co-O-Ru antiferromagnetic sublattice. Below its ordering temperature ($\sim 150\text{K}$), the ferromagnetic Ru sublattice polarizes the paramagnetic Co moments in a direction opposite to the applied field leading to magnetic compensation and negative magnetization. Once the Co moments align antiferromagnetically below the antiferromagnetic ordering temperature of Co-O-Ru sublattice ($\sim 80\text{K}$) the magnetization increases towards a positive value as can be seen in Fig. 7(d).

LaSrCoRuO $_6$ is AA'BB'O $_6$ type double perovskite crystallizing in a monoclinic structure. This structure allows for ordering of B-site cations in a NaCl

fashion. This ordering is favoured due to the charge difference ($\Delta q \geq 3$) between Co and Ru. In perfectly ordered LaSrCoRuO_6 , Co^{2+} and Ru^{5+} magnetic ions couple antiferromagnetically leading to an antiferromagnetic ground state as can be seen from neutron diffraction measurements. A disorder in Co and Ru site occupancy will result in Ru-O-Ru type linkages which are known to align ferromagnetically. The presence of ferromagnetic interactions is clearly visible in LSCR12 which has a larger B-site occupancy disorder in terms of increased values of magnetization as compared to those in LSCR13 and hysteresis in M vs H loop. Due to such a disorder in occupancy of Co and Ru sites, octahedral distortions set in, as the immediate neighbour of a Ru octahedra could be either a Ru octahedra or a Co octahedra. EXAFS results in LSCR12 bear a testimony to this fact. In LSCR12, the Co-O and Ru-O bond lengths are shorter, the mean square displacement is higher and Co-O-Ru bond is straighter. These changes are a result of Ru-O-Ru ferromagnetic linkages which due to their presence alter Ru-O-Co antiferromagnetic interactions. The negative magnetization seen in the low field ZFC magnetization is due to Ru-O-Ru ferromagnetic interactions which below $\sim 150\text{K}$ polarize the paramagnetic Co spins in a the direction opposite to applied field giving rise to magnetic compensation.

4 Conclusions

The disorder in occupation of Co and Ru sites in LaSrCoRuO_6 double perovskite results in Ru-O-Ru linkages which are ferromagnetic. Due to such linkages, the magnetization of disordered compound increases in magnitude as compared to that of ordered compound. At low applied fields the ferromagnetic spins polarize the paramagnetic Co spins in a direction opposite to the direction of magnetic field resulting in observed negative magnetization.

Acknowledgements

KRP and PRS would like to thank Department of Science and Technology (DST), Government of India for financial support under the project No. SR/S2/CMP-42. PSRM acknowledges support from UGC-DAE Consortium for Scientific Research, Mumbai Centre for financial support under CRS-M-126. KRP would also like to thank DST for travel funding under Utilization of International Synchrotron Radiation and Neutron Scattering facilities.

References

- [1] K. L. Kobayashi, T. Kimura, H. Sawada, K. Terakura and Y. Tokura, Nature (London) **395**, 677 (1998).
- [2] J. Gopalakrishnan, A. Chattopadhyay, S. B. Ogale, T. Venkatesan, R. L. Greene, A. J. Millis, K. Ramesha, B. Hannoyer and G. Marest, Phys. Rev. B **62**, 9538 (2000).
- [3] D. D. Sarma, Curr. Opin. Solid State Mater. Sci. **5**, 261 (2001).
- [4] A. A. Taskin and Y. Ando, Phys. Rev. Lett. **98**, 207201 (2007).
- [5] K. P. Belov, Phys. Usp. **39**, 623 (1996); **42**, 711 (1999); **43**, 407 (2000).
- [6] Y. Ren, T. T. M. Palstra, D. I. Khomskii, E. Pellegrin, A. A. Nugroho, A. A. Menovsky and G. Sawatzky, Nature **396**, 441 (1998).
- [7] Y. Ren, T. T. M. Palstra, D. I. Khomskii, A. A. Nugroho, A. A. Menovsky and G. Sawatzky, Phys. Rev. B **62**, 6577 (2000).
- [8] K. Yoshii, J. Solid State Chem. **159**, 204 (2001).
- [9] K. Yoshii, A. Nakamura, A. Ishii and Y. Morii, J. Solid State Chem. **162**, 84 (2001).
- [10] R. P. Singh and C. V. Tomy, Phys. Rev. B **78**, 024432 (2008).
- [11] R. P. Singh and C. V. Tomy, J. Phys.: Condens. Matter **20**, 235209 (2008).
- [12] G. Cao, Y. Xin, C. S. Alexander, and J. E. Crow, Phys. Rev. B **63**, 184432 (2001).
- [13] J-W. G. Bos, J. P. Attfield, Chem. Matter. **16**, 1822 (2004).
- [14] A. Mamchik, W. Dmowski, T. Egami, I-W. Chen, Phys. Rev. B **70**, 104410 (2004).
- [15] S. H. Kim, P. D. Battle, J. Sol. State Chem. **114**, 174 (1995).
- [16] S. Kim, R. I. Dass and J. B. Goodenough, J. Sol. State Chem. **181**, 2989 (2008).
- [17] P. Tomeš, J. Hejtmánek and K. Knížek, Sol. State Sci. **10**, 486 (2008).

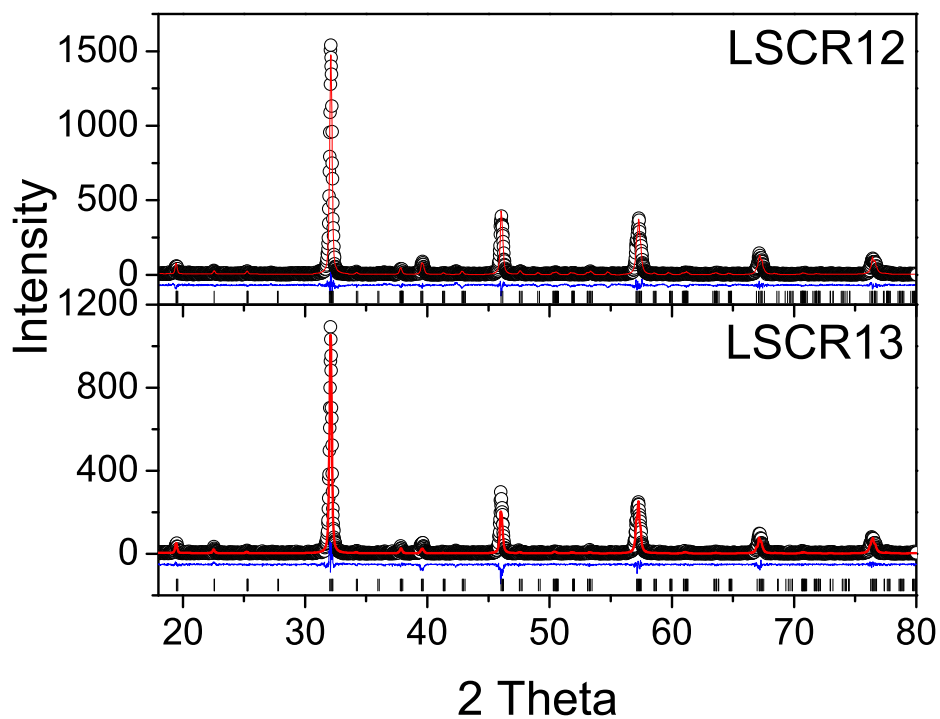


Fig. 1. Rietveld refined XRD patterns for LSCR13 and LSCR12. The open circles show the observed counts and the continuous line passing through these counts is the calculated profile. The difference between the observed and calculated patterns is shown as a continuous line at the bottom of the two profiles. The calculated positions of the reflections are shown as vertical bars.

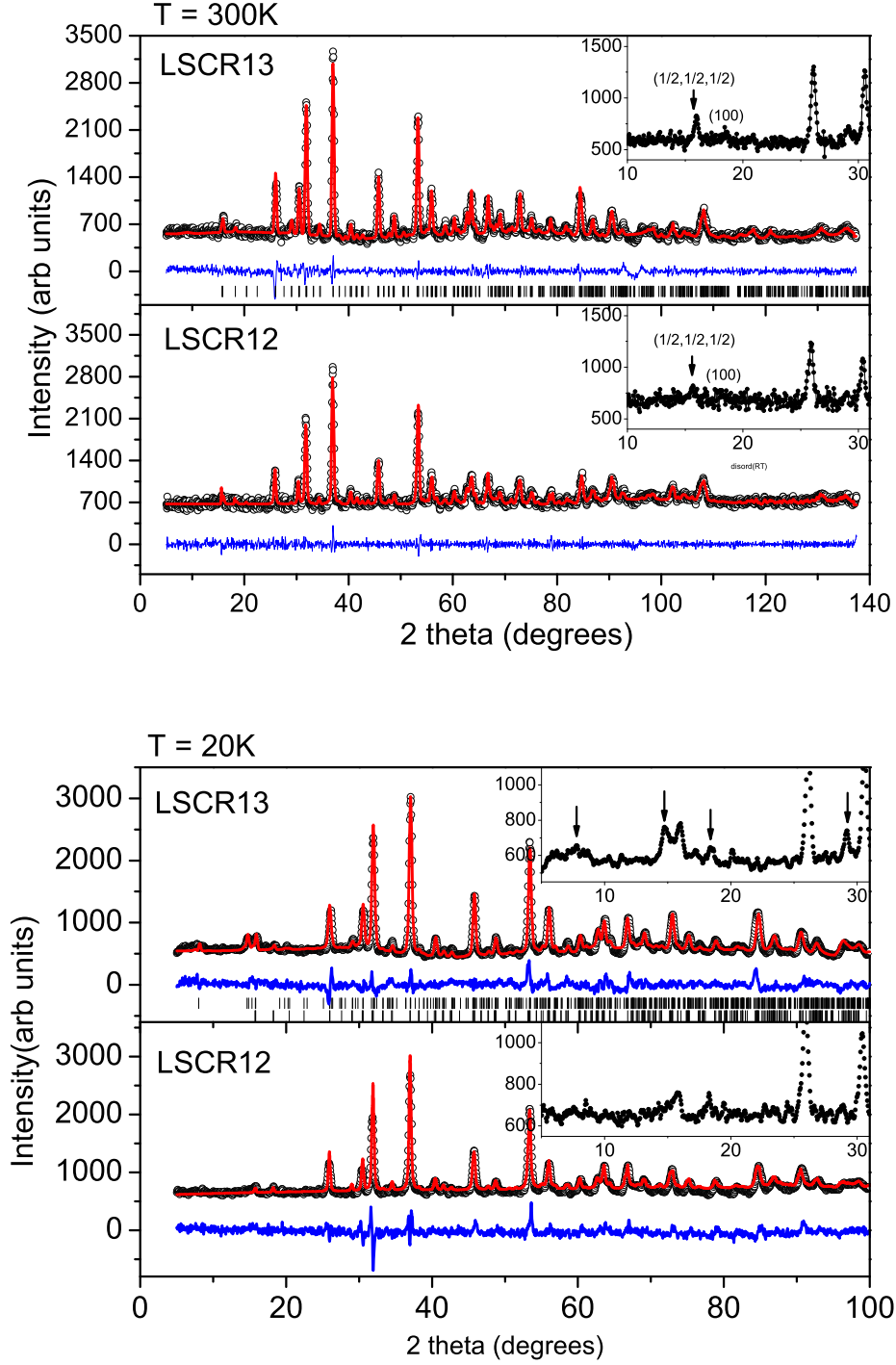


Fig. 2. Observed (circles), calculated (line) and difference ND patterns recorded at 300K (upper panel) for LSCR13 and LSCR12. The inset presents data in limited range with the superlattice reflections seen clearly in LSCR13 indicating higher degree of order. The lower panel shows neutron data taken at 20K for the same samples. The inset presents data in limited range with the arrows indicating magnetic reflections present in LSCR13.

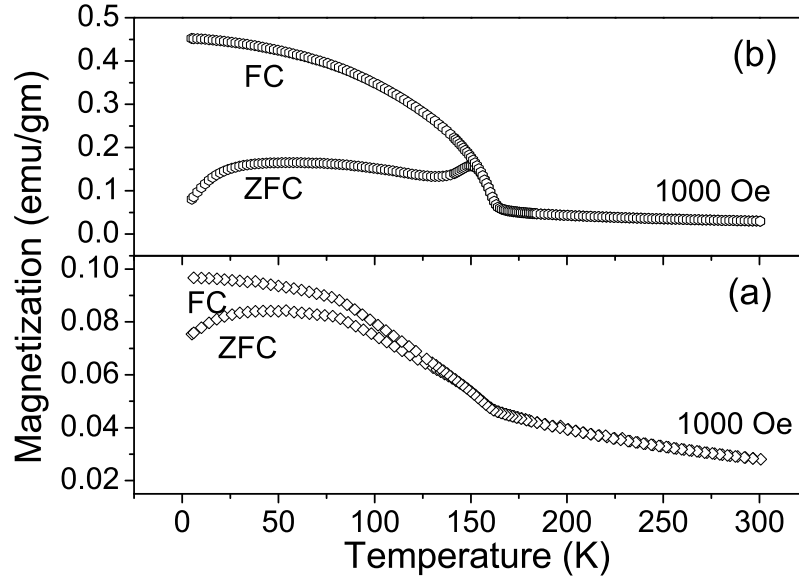


Fig. 3. Magnetization as a function of temperature at applied fields of 1000 Oe in LSCR13 (a) and LSCR12 (b).

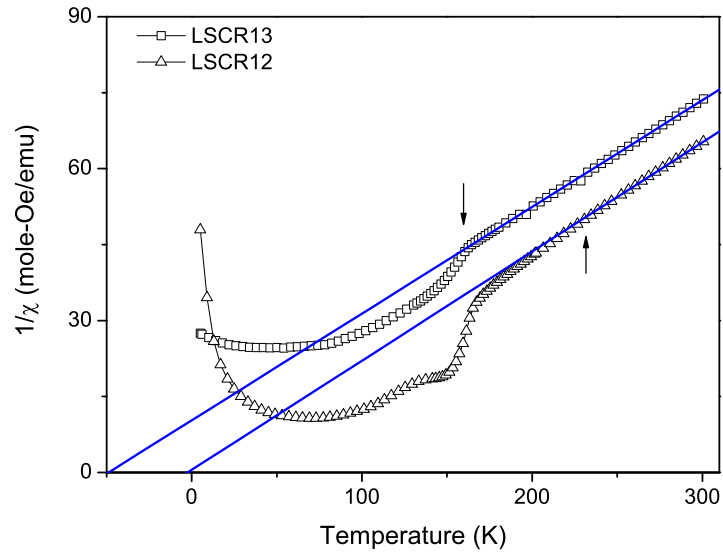


Fig. 4. Inverse Magnetic susceptibility function of temperature calculated as $\chi = M/H$ at applied fields of 1000 Oe in LSCR13 and LSCR12.

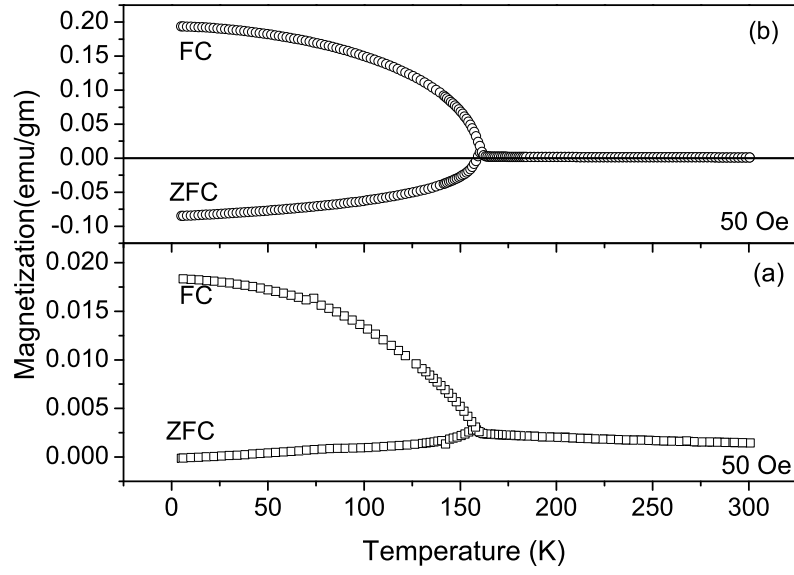


Fig. 5. ZFC and FC magnetization curves at applied field of 50 Oe recorded for LSCR13 (a) and LSCR12 (b).

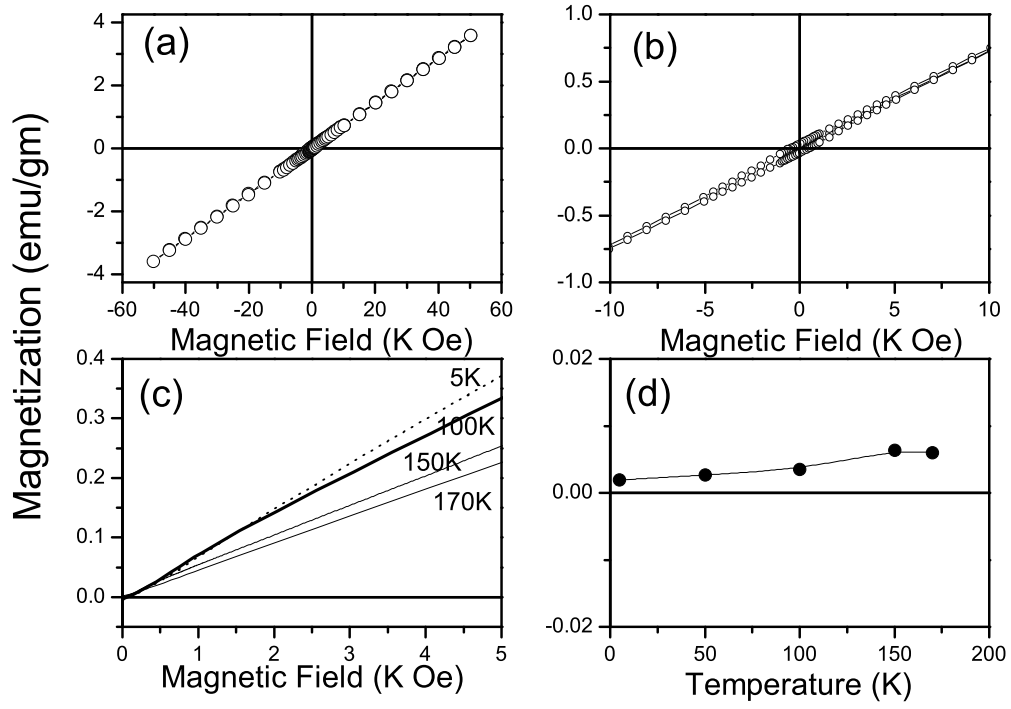


Fig. 6. Isothermal magnetization curves for LSCR13 recorded in the field interval of ± 5 T at 5K (a); its magnified view (± 10 KOe) (b); virgin magnetization curves at few representative temperatures (c) and variation of magnetization values extracted from virgin curves at a field value of *sim* 50 Oe.

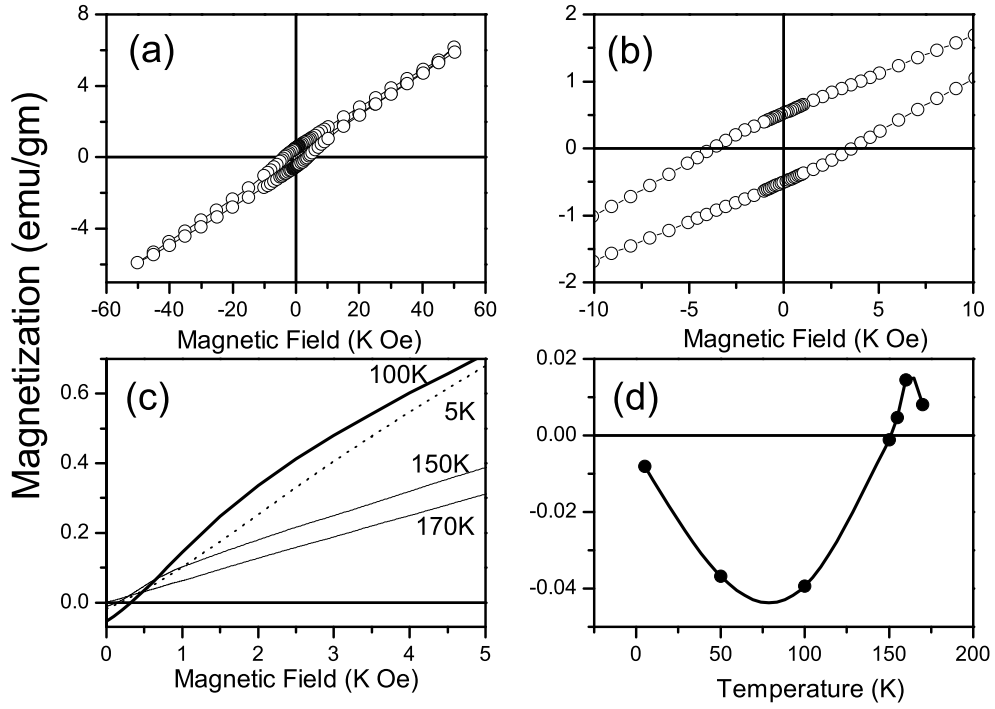


Fig. 7. Isothermal magnetization curves for LSCR12 recorded in the field interval of ± 5 T at 5K (a); its magnified view (± 10 KOe) (b); virgin magnetization curves at few representative temperatures (c) and variation of magnetization values extracted from virgin curves at a field value of ~ 50 Oe.

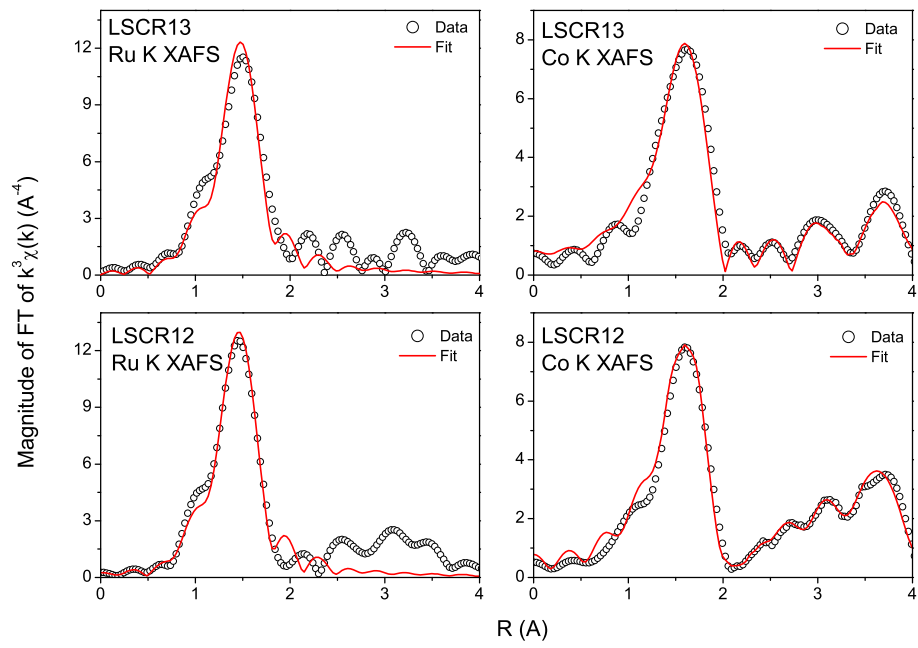


Fig. 8. k^3 weighted magnitude of Fourier transform of EXAFS data recorded at Co and Ru K-edge in LSCR13 and LSCR12.